THE JOURNAL OF BIOLOGICAL CHEMISTRY VOL. 286, NO. 32, pp. 28138–28149, August 12, 2011


# G Protein Binding Sites on Calnuc (Nucleobindin 1) and NUCB2 (Nucleobindin 2) Define a New Class of Gα$_i$-regulatory Motifs*[S]

Received for publication, November 17, 2010, and in revised form, June 4, 2011 Published, JBC Papers in Press, June 8, 2011, DOI 10.1074/jbc.M110.204099

**Mikel Garcia-Marcos**[‡1], **Patrick S. Kietrsunthorn**[‡], **Honghui Wang**[‡], **Pradipta Ghosh**[§2], **and Marilyn G. Farquhar**[‡3]

*From the Departments of* [‡]*Cellular and Molecular Medicine and* [§]*Medicine, University of California, San Diego, La Jolla, California 92093*

**Heterotrimeric G proteins are molecular switches modulated by families of structurally and functionally related regulators. GIV (Gα-interacting vesicle-associated protein) is the first non-receptor guanine nucleotide exchange factor (GEF) that activates Gα$_i$ subunits via a defined, evolutionarily conserved motif. Here we found that Calnuc and NUCB2, two highly homologous calcium-binding proteins, share a common motif with GIV for Gα$_i$ binding and activation. Bioinformatics searches and structural analysis revealed that Calnuc and NUCB2 possess an evolutionarily conserved motif with sequence and structural similarity to the GEF sequence of GIV. Using *in vitro* pulldown and competition assays, we demonstrate that this motif binds preferentially to the inactive conformation of Gα$_{i1}$ and Gα$_{i3}$ over other Gα subunits and, like GIV, docks onto the α3/switch II cleft. Calnuc binding was impaired when Lys-248 in the α3 helix of Gα$_{i3}$ was replaced with M, the corresponding residue in Gα$_o$, which does not bind to Calnuc. Moreover, mutation of hydrophobic residues in the conserved motif predicted to dock on the α3/switch II cleft of Gα$_{i3}$ impaired the ability of Calnuc and NUCB2 to bind and activate Gα$_{i3}$ *in vitro*. We also provide evidence that calcium binding to Calnuc and NUCB2 abolishes their interaction with Gα$_{i3}$ *in vitro* and in cells, probably by inducing a conformational change that renders the Gα$_i$-binding residues inaccessible. Taken together, our results identify a new type of Gα$_i$-regulatory motif named the GBA motif (for Gα-binding and -activating motif), which is conserved across different proteins throughout evolution. These findings provide the structural basis for the properties of Calnuc and NUCB2 binding to Gα subunits and its regulation by calcium ions.**

Recently it has become clear that in addition to G protein-coupled receptors and Gβγ subunits, the function of the Gα subunits of heterotrimeric G proteins is controlled by accessory proteins that regulate their activity and/or localization (1–3). The first group of such regulators to be described was the regulators of G protein signaling (RGS)[4] protein family, which serve as GTPase-activating proteins for Gα$_i$, Gα$_q$, and Gα$_{12}$ subunits via a 120-aa conserved domain, the "RGS box" (4, 5). Subsequent studies revealed another group of regulatory proteins with GDI activity for Gα$_i$ subunits, which have a common signature motif, *i.e.* the GoLoco or G protein-regulatory (GPR) motif (1, 6, 7). Both the RGS box (8, 9) and the GoLoco/GPR motif (10) have been structurally resolved by X-ray chrytallography, and their critical roles in metabolism, cell division, and cardiovascular function, among others, have made them emerging pharmacological targets (11, 12). We recently described another Gα-interacting protein, GIV (13), and showed that it is a GEF that activates Gα subunits and mediates its biological functions via a defined motif (14) with structural similarity to the synthetic GEF peptide KB-752 (15). GIV is a metastasis-related protein (16) that enhances PI3K-Akt signaling and promotes macrophage, endothelial, epithelial, and tumor cell migration (17–19).

We identified Calnuc (nucleobindin 1 or NUCB1) as a Gα-binding protein in a yeast two-hybrid screen using Gα$_{i3}$ as bait (21). Calnuc, the most abundant protein in the Golgi (24) and the major calcium-binding protein within the Golgi lumen (21–23), regulates intracellular calcium stores via its two EF-hands (22). In addition, we have shown previously that there is a significant soluble pool of Calnuc in the cytosol (21, 25), which interacts with Gα$_{i3}$ *in vivo* on the surface of Golgi membranes as demonstrated by FRET and live cell imaging (26). The role of cytosolic Calnuc as a G protein regulator was further substantiated by the finding that it controls the intracellular localization of Gα$_i$ subunits in neuroendocrine cells (27). However, the mechanism by which Calnuc binds or regulates Gα$_i$ subunits remains unknown. Here we identified a conserved motif in Calnuc and the highly homologous protein NUCB2 (nucleobindin 2 or NEFA) (20) with similarity to the GEF motif of GIV and characterized how this motif binds and regulates Gα$_i$ subunits. These findings help define a new class of structurally defined G

* This work was supported, in whole or in part, by National Institutes of Health Grants DKI7780 and CA100768 (to M. G. F.).
[S] The on-line version of this article (available at http://www.jbc.org) contains supplemental Figs. S1–S5.
[1] Supported by Postdoctoral Fellowship KG080079 from the Susan G. Komen Foundation.
[2] Supported by a Career Award for Medical Scientists (CAMS) from the Burroughs Wellcome Fund and a Research Scholar Award from the American Gastroenterology Association.
[3] To whom correspondence should be addressed: Dept. of Cellular and Molecular Medicine, George Palade Laboratories of Cellular and Molecular Medicine, University of California, San Diego, 9500 Gilman Dr., La Jolla, CA 92093-0651. Tel.: 858-534-7711; Fax: 858-534-8549; E-mail: mfarquhar@ucsd.edu.

[4] The abbreviations used are: RGS, regulator of G protein signaling; GIV, Gα-interacting vesicle-associated protein; GEF, guanine nucleotide exchange factor; GDI, guanine nucleotide dissociation inhibitor; GPR, G protein-regulatory; aa, amino acid(s); GBA, Gα binding and activating; GTPγS, guanosine 5′-3-*O*-(thio)triphosphate; SwII, switch II; CFP, cyan fluorescent protein; GSP, Galphas(s)-binding peptide.

protein regulatory motifs and provide insights into how the interaction between Gα$_{i3}$ and Calnuc is regulated.

## EXPERIMENTAL PROCEDURES

*Reagents and Antibodies*—The peptide corresponding to the Calnuc Gα$_i$-binding motif, *i.e.* $^{309}$RLVTLEEFLASTQRKE$^{324}$ (Calnuc-(309–324) peptide, >95% purity), was synthesized and purified as described (28). The control peptide (EVVTLQQ*A*LEESNKLT, >95% purity) used in our experiments, corresponding to the GEF sequence of GIV with a F1685A mutation that abolishes binding and GEF activity (14), was custom-made by Genway Biotech (San Diego). NUCB2 cDNA was obtained from Open Biosystems. The sources of the remainder of the reagents and antibodies used were described previously (14, 17, 29).

*Plasmid Constructs, Mutagenesis, and Protein Expression*—Cloning of GST- or His-tagged Gα$_{i1}$, Gα$_{i2}$, Gα$_{i3}$, and Gα$_o$ was described previously (14, 29). Full-length rat Calnuc and NUCB2-(173–333), containing the putative Gα-binding motif, were inserted between the BamHI and XhoI restriction sites of the pGEX-4T-1 vector to generate GST-Calnuc and GST-NUCB2, respectively. His-tagged full-length Calnuc-(1–459) and Calnuc-(171–459) (CalnucΔN) and full-length rat NUCB2 were cloned using the ligation-independent cloning vector pMCSG7 exactly as described previously (30). Cloning of rat Gα$_{i3}$ with three FLAG sequences fused to the C terminus of the protein (Gα$_{i3}$-FLAG) using the mammalian expression vector p3XFLAG-CMV-14 was described previously (29). Cloning Calnuc into pcDNA3.1 with a CFP fused at the C terminus and lacking the signal sequence (aa 2–25, ΔSS-Calnuc-CFP) was described previously (26). Calnuc, NUCB2, and Gα$_{i3}$ mutants were generated using specific primers (sequences available upon request) following the manufacturer's instructions (QuikChange II, Stratagene, San Diego). Purification of GST- or His-tagged Gα$_{i1}$, Gα$_{i2}$, Gα$_{i3}$, and Gα$_o$ was carried out following described protocols (14, 17, 29). A modified protocol was used for the purification of GST-Calnuc, His-Calnuc, His-CalnucΔN, His-NUCB2, and GST-NUCB2. Briefly, induction of protein expression for these constructs was carried out using the autoinduction protocol described by Studier (31). Briefly, BL21(DE3) cells were incubated at 37 °C for 5 h (~$A_{600}$ = 0.6–0.8), switched to 23 °C for 19 h, and harvested at $A_{600}$ = 5–15. Cell lysis was carried out in a French press, and the remainder of the purification was performed as described (14, 17, 29) with an additional purification step by gel filtration chromatography using a Superdex 200 column attached to an AKTA FPLC machine. Fractions containing the protein of interest were pooled and in some cases concentrated using an Amicon Ultra filter (10,000 Da cut-off, Millipore). His-NUCB2 was toxic in *Escherichia coli*, resulting in slow growth and low yields of protein (~0.3 mg/liter bacterial culture) compared with His-Calnuc (~3 mg/liter bacterial culture), His-CalnucΔN (~10–15 mg/liter bacterial culture), or GST-NUCB2-(173–333) (~8 mg/liter bacterial culture).

*In Vitro Protein Binding (Pulldown) Assays*—This assay was performed essentially as described previously (14, 17, 29). Briefly, purified GST fusion proteins or GST alone (3–20 μg) was immobilized on glutathione-Sepharose beads and incubated in binding buffer (50 mM Tris-HCl, pH 7.4, 100 mM NaCl, 0.4% (v:v) Nonidet P-40, 10 mM $MgCl_2$, 5 mM EDTA, 2 mM DTT, and protease inhibitor mixture) containing either 30 μM GDP or 30 μM GDP, 30 μM $AlCl_3$, and 10 mM NaF or 30 μM GTPγS for 90 min at room temperature. Solubilized proteins from ~750 μg rat brain membranes or 2–6 μg purified His-tagged proteins were added to each tube, and binding reactions were carried out overnight at 4 °C with constant tumbling. Beads were washed four times with 1 ml of wash buffer (4.3 mM $Na_2HPO_4$, 1.4 mM $KH_2PO_4$, pH 7.4, 137 mM NaCl, 2.7 mM KCl, 0.1% (v:v) Tween 20, 10 mM $MgCl_2$, 5 mM EDTA, and 2 mM DTT supplemented with GDP, GDP plus $AlCl_3$, and NaF or GTPγS as during binding) and boiled in sample buffer for SDS-PAGE.

*Immunoblotting*—Proteins samples were separated on 10% SDS-PAGE and transferred to PVDF membranes (Millipore, Billerica, MA). In experiments using His-Calnuc, His-CalnucΔN, or His-NUCB2 all electrophoretic steps were performed in the presence of 4 M urea, which increased the sensitivity of the immunodetection. Membranes were blocked with PBS supplemented with 5% nonfat milk before sequential incubation with primary and secondary antibodies. Infrared imaging was performed using an Odyssey imaging system (LI-COR Biosciences, Lincoln, NE). Primary antibodies were diluted as follows: anti-His, 1:2000; anti-Gα$_{i3}$, 1:300, anti-Gα$_o$, 1:500; anti-Gα$_s$, 1:250.

*Steady-state GTPase Assay*—This assay was performed as described previously (14, 29). Briefly, His-Gα$_{i3}$ (100 nM) was preincubated with different concentrations of His-CalnucΔN-(171–459) or GST-NUCB2 (173–333) for 15–30 min at 30 °C in assay buffer (20 mM Na-HEPES, pH 8, 100 mM NaCl, 1 mM EDTA, 2 mM $MgCl_2$, 1 mM DTT, and 0.05% (w:v) C12E10). His-CalnucΔN and GST-NUCB2-(173–333) were used instead of full-length His-Calnuc or GST-NUCB2 because the protein concentrations used in these experiments were achievable for only the truncated proteins, which express at higher yields in bacteria. GTPase reactions were initiated at 30 °C by adding an equal volume of assay buffer containing 1 μM [γ-$^{32}$P]GTP (~50 cpm/fmol). Duplicate aliquots (50 μl) were removed at different time points, and reactions were stopped with 950 μl of ice-cold 5% (w/v) activated charcoal in 20 mM $H_3PO_4$, pH 3. Samples were then centrifuged for 10 min at 10,000 × *g*, and 500 μl of the resultant supernatant was scintillation-counted to quantify released [$^{32}$P]$P_i$. To determine the specific $P_i$ produced, the background [$^{32}$P]$P_i$ detected at 10 min in the absence of G protein was subtracted from each reaction.

*GTPγS Binding Assay*—GTPγS binding was measured using a filter binding method. His-Gα$_{i3}$ (100 nM) was preincubated in the presence or absence of 45 μM His-CalnucΔN for 30 min at 30 °C in assay buffer (20 mM Na-HEPES, pH 8, 100 mM NaCl, 1 mM EDTA, 25 mM $MgCl_2$, 1 mM DTT, and 0.05% (w:v) C12E10). Reactions were initiated at 30 °C by adding an equal volume of assay buffer containing 1 μM [$^{35}$S] GTPγS (~50 cpm/fmol). Duplicate aliquots (25 μl) were removed at different time points, and binding of radioactive nucleotide was stopped by the addition of 3 ml of ice-cold wash buffer (20 mm Tris-HCl, pH 8.0, 100 mm NaCl, and 25 mm $MgCl_2$). The quenched reactions were rapidly passed through BA-85 nitrocellulose filters

(GE Healthcare) and washed with 4 ml of wash buffer. Filters were dried and subjected to liquid scintillation counting. Experiments designed to study the effect of $Ca^{2+}$ were performed as described above except that no EDTA was used and different concentrations of $CaCl_2$ were added.

*Cell Culture, Transfection, and Immunoprecipitation*—COS-7 cells were grown at 37 °C in DMEM supplemented with 10% FBS, 100 units/ml penicillin, 100 μg/ml streptomycin, 1% L-glutamine, and 5% $CO_2$ and transfected with plasmids encoding for ΔSS-Calnuc-CFP (lacking the signal sequence; aa 2–25, 0.5 μg) and Gα$_{i3}$-FLAG (6 μg) or vector control (6 μg) using GeneJuice as described previously (29). 36 h after transfection the cells were maintained overnight in DMEM alone (~1.8 mM calcium) and then stimulated or not with 1 μM thapsigargin or 100 μM ATP for 90 s, rinsed quickly twice with ice-cold PBS, scraped into lysis buffer (20 mM HEPES, pH 7.2, 5 mM $Mg(CH_3COO)_2$, 125 mM $K(CH_3COO)$, 0.4% Triton X-100, and 1 mM DTT) supplemented with phosphatase (Sigma) and protease (Roche Applied Science) inhibitor mixtures, passed through a 28-gauge needle at 4 °C, and cleared (10,000 × *g* for 10 min). COS-7 cell lysates (~1–2 mg) were incubated for 2.5 h at 4 °C with 2 μg anti-FLAG mAb (Sigma) followed by incubation with protein G-agarose beads (GE Healthcare) at 4 °C for an additional 45 min. Beads were washed four times with 1 ml of wash buffer (4.3 mM $Na_2HPO_4$, 1.4 mM $KH_2PO_4$, pH 7.4, 137 mM NaCl, 2.7 mM KCl, 0.1% (v:v) Tween 20, 10 mM $MgCl_2$, 5 mM EDTA, and 2 mM DTT), and the bound immune complexes were eluted by boiling in SDS sample buffer.

*Preparation of Detergent-soluble Extracts from Rat Brain Membranes*—Isolation of rat brain membranes was adapted from a fractionation procedure described previously for liver (32). Briefly, rat brains were homogenized in 10 mM HEPES-KOH, pH 7.4, 5 mM EDTA, and 0.5 M sucrose with a Teflon-glass homogenizer and spun down at 1,000 × *g* for 10 min to sediment unbroken tissue and nuclei, and the resulting supernatant (postnuclear supernatant) was collected. Crude membranes were sedimented from the postnuclear supernatant by centrifugation at 100,000 × *g*, aliquoted, and stored at −80 °C. Rat brain membrane lysates were freshly prepared prior to the pulldown experiments presented in Fig. 4 by solubilizing ~750 μg of protein/condition in binding buffer (50 mM Tris-HCl, pH 7.4, 100 mM NaCl, 0.4% (v:v) Nonidet P-40, 10 mM $MgCl_2$, 5 mM EDTA, 2 mM DTT, and protease inhibitor mixture) for ~2 h at 4 °C. Lysates were cleared (14,000 × *g* for 10 min) before use in subsequent experiments.

*Other Methods*—Protein structure analysis and visualization was performed using ICM-Browser-Pro software (Molsoft Inc., San Diego). Data presented in Figs. 2*C*, 7*C*, and 8*D* and supplemental Fig. S4 were curve-fitted by nonlinear regression using Prism 4.0. (San Diego) to determine the $K_d$, $EC_{50}$, and $IC_{50}$ values.

## RESULTS

*Identification of a Putative Gα-interacting Motif in Calnuc and NUCB2*—By manual examination of the Calnuc sequence, we noticed a region with significant similarity to the GEF motif of GIV and two synthetic peptides with GEF activity, KB-752 (15) and GSP (33) (Fig. 1*A*). This motif (aa 309–324) overlaps

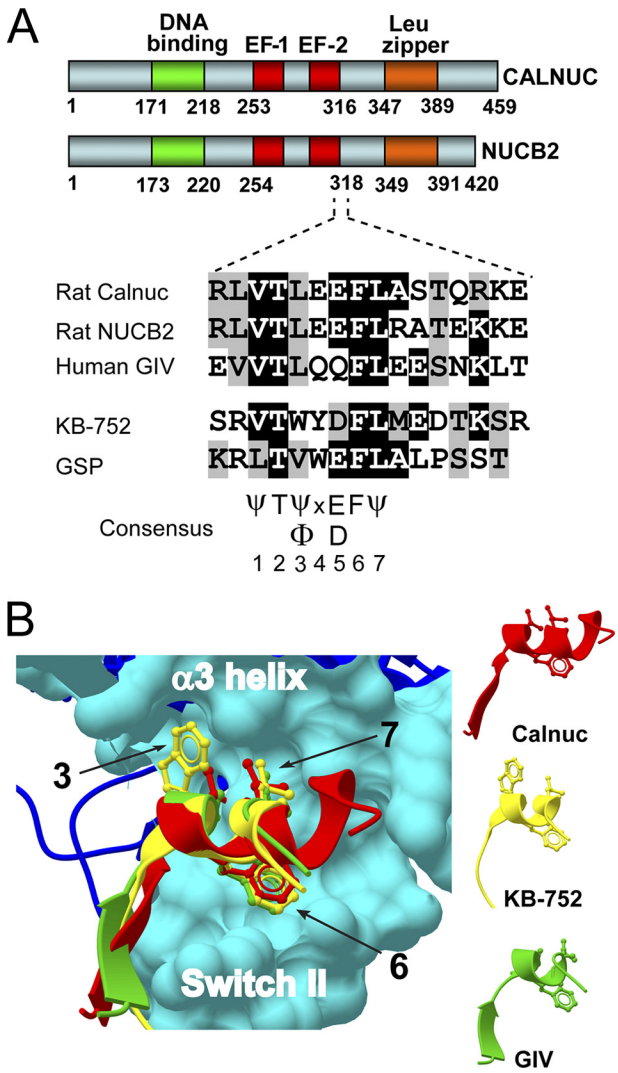


FIGURE 1. **Identification of a putative Gα-binding motif in Calnuc and NUCB2.** *A*, a sequence at the end of the Calnuc (aa 309–324) and NUCB2 (aa 311–326) second EF-hand shows a similarity to the GEF motif of GIV (aa 1678–1693) and the synthetic KB-752 and GSP peptides. Rat Calnuc, rat NUCB2, and human GIV sequences were obtained from the NCBI and aligned with the KB-752 (15) and GSP (33) sequences using ClustalW. Conserved identical residues are shaded in *black* and similar residues in *gray*. A consensus sequence of 7 aa based on this alignment and the phylogenetic analysis of Calnuc (Fig. S1) and GIV (14) is indicated. *B*, the Calnuc putative Gα$_i$-binding motif has a structural similarity to the KB-752 peptide and the GEF motif of GIV. The coordinates of the Calnuc putative Gα-binding sequence (aa 309–320 (*red*)) were extracted from the Protein Data Bank (ID code: 1SNL) and the coordinates for the GEF motif of GIV (aa 1678–1689 (*green*)) from a previously described homology model (14). Both were threaded over the structure of KB-752 (*yellow*) in complex with Gα$_{i1}$ (*blue*) (Protein Data Bank ID code: 1Y3A) using ICM-Browser-Pro. The Calnuc putative Gα$_i$-binding motif, the GEF motif of GIV, and KB-752 form a helix in which the side chains of hydrophobic residues corresponding to positions 3, 6, and 7 from the consensus sequence depicted in *A* dock onto the α3/SwII hydrophobic cleft of the Gα$_i$ subunits (*cyan* surface).

with the C-terminal part of the second EF-hand of Calnuc and is also found in NUCB2, a protein highly homologous to Calnuc (62% aa sequence identity). Phylogenetic analysis revealed that this motif is evolutionarily conserved in both Calnuc and NUCB2 proteins from invertebrates to humans (supplemental Fig. S1). In addition, the structure of this motif extracted from the NMR coordinates of the calcium-binding domain of Calnuc (34) is very similar to the established crystal structure of the

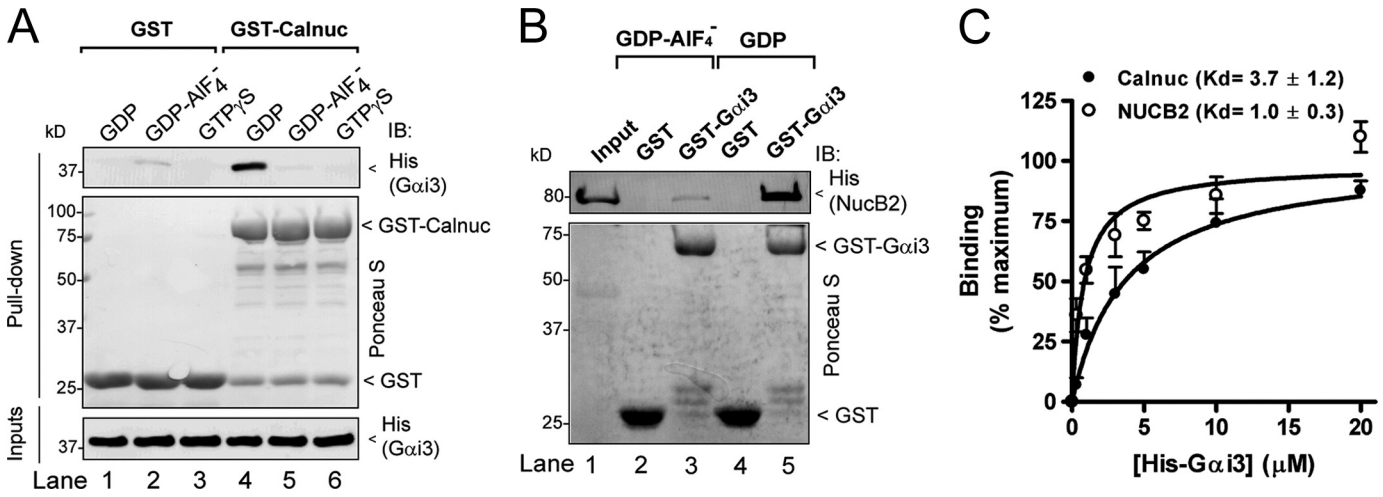


FIGURE 2. **Calnuc and NUCB2 bind inactive but not active Gα$_{i3}$.** *A*, His-Gα$_{i3}$·GDP (*lane 4*) but not His-Gα$_{i3}$·GDP·AlF$_4^-$ (*lane 5*) or His-Gα$_{i3}$·GTPγS (*lane 6*) binds to GST-Calnuc. No binding of Gα$_{i3}$ to GST was detected under any of the conditions tested (*lanes 1–3*). 6 μg of His-Gα$_{i3}$ preloaded with GDP (*lanes 1* and *4*), GDP and AlF$_4^-$ (*lanes 2* and *5*), or GTPγS (30 μM, *lanes 3* and *6*) were incubated with ~20 μg of purified GST (*lanes 1–3*) or GST-Calnuc (*lanes 4–6*) immobilized on glutathione beads. After extensive washing, bound proteins were separated by SDS-PAGE and analyzed by immunoblotting (*IB*) for His. Equal loading of GST proteins was confirmed by Ponceau S staining (*middle panel*), and equal loading of His-Gα$_{i3}$ by His immunoblotting (*lower panel*). *B*, GST-Gα$_{i3}$·GDP (*lane 5*) but not GST-Gα$_{i3}$·GDP·AlF$_4^-$ (*lane 3*) or GST (*lanes 2* and *4*) binds His-NUCB2. 10 μg of His-NUCB2 was incubated with ~15 μg of purified GST (*lanes 2* and *4*) or GST-Gα$_{i3}$ (*lanes 3* and *5*) preloaded with GDP (*lanes 4* and *5*) or GDP·AlF$_4^-$ (*lanes 2* and *3*) immobilized on glutathione beads and analyzed as described in *A*. *Input* (*lane 1*), 1 μg of His-NUCB2. *C*, His-Gα$_{i3}$·GDP binds to GST-Calnuc and GST-NUCB2-(173–333) with a $K_d$ of 3.7 ± 1.2 μM ($n$ = 4) and 1.0 ± 0.3 μM ($n$ = 3), respectively. Increasing concentrations of His-Gα$_{i3}$·GDP (0.3, 0.5, 1, 1.5, 3, 5, 10, and 20 μM) were incubated with 20 μg of GST-Calnuc (*closed circles*) or GST-NUCB2 (*open circles*) and analyzed as in *A*. His-Gα$_{i3}$ binding was determined by quantitative immunoblotting using an Odyssey infrared imaging system, and data were fitted to a nonlinear, one-site binding hyperbola (*solid lines*) using Prism 4.0.

KB-752 peptide bound to Gα$_{i1}$ (15) and the homology-based structural prediction for the GEF motif of GIV bound to Gα$_{i3}$ (14) (Fig. 1*B*). These observations indicate that Calnuc and NUCB2 possess an evolutionarily conserved motif with structural similarity to the GEF motif of GIV and GIV-related peptides that display GEF activity.

*Calnuc and NUCB2 Bind Preferentially to Inactive Gα$_{i3}$*—Based on the sequence and structural similarities described above, we reasoned that Calnuc and NUCB2 might have similar Gα binding properties to those of the GEF motif of GIV and related peptides that bind specifically to inactive GDP-bound Gα$_i$ subunits. We found that this was indeed the case for both Calnuc (Fig. 2*A*) and NUCB2 (Fig. 2*B*). GST-Calnuc bound robustly to inactive, GDP-loaded His-Gα$_{i3}$ but not to the G protein when it was activated by either GDP·AlF$_4^-$ or GTPγS loading (Fig. 2*A*). Similar results (data not shown) were obtained in pulldown assays using GST-Gα$_{i3}$ and His-tagged Calnuc or CalnucΔN-(171–459), an N-terminally truncated construct containing the putative Gα-binding motif. Similarly, His-NUCB2 showed robust binding to GST-Gα$_{i3}$ in the presence of GDP but not in the presence of GDP·AlF$_4^-$ (Fig. 2*B*). The interaction of GST-Calnuc and GST-NUCB2-(173–333) (containing the putative Gα-binding motif), with GDP-loaded His-Gα$_{i3}$, has a dissociation constant ($K_d$) of 3.7 ± 1.2 and 1.0 ± 0.3 μM, respectively (Fig. 2*C*). These results indicate that, much like GIV and the GIV-related peptides, binding of Calnuc and NUCB2 to Gα$_{i3}$ is state-dependent with a marked preference for the inactive conformation.

*Calnuc and NUCB2 Bind to the α3/Switch II Cleft on Gα$_i$·GDP*—Next we performed competition assays to determine whether Calnuc and NUCB2 shared a common binding site on Gα$_{i3}$ with the synthetic KB-752 peptide and GIV, which bind to the hydrophobic cleft circumscribed by the α3 helix and "switch II" (SwII) (14, 15). We found that increasing concentrations of KB-752, but not a control peptide (see "Experimental Procedures"), decreased His-Gα$_{i3}$ binding to GST-Calnuc (Fig. 3*A*). Similarly, increasing concentrations of a peptide (aa 309–324) corresponding to the putative Gα$_i$ binding sequence of Calnuc, but not a control peptide, decreased the amount of His-GIV-CTs (aa 1660–1870, containing the GEF motif of GIV) that bound to GST-Gα$_{i3}$ (Fig. 3*B*). We also performed similar competition assays with GST-NUCB2-(173–333) and found that it also competed with the KB-752 peptide (Fig. 3*C*) or His-GIV-CTs (Fig. 3*D*) but not with their respective controls for binding to Gα$_{i3}$. Taken together these results suggest that Calnuc and NUCB2 bind specifically to the α3/SwII cleft of Gα$_{i3}$·GDP via the newly identified motif.

*Characterization of Calnuc Specificity for Gα Subunits*—We have previously shown that Calnuc can interact with Gα$_i$, Gα$_o$, and Gα$_s$ but not Gα$_{12/13}$ or Gα$_q$ in yeast two-hybrid assays (21). Next we investigated the relative strength of the interaction of Calnuc with Gα$_i$, Gα$_o$, and Gα$_s$ using *in vitro* protein-protein binding assays. We found that GST-Calnuc bound GDP-loaded Gα$_{i3}$ from rat brain membrane lysates, whereas binding of Gα$_o$ was very weak and binding of Gα$_s$ was undetectable (Fig. 4*A*). We further performed pulldown assays using purified GST-Gα$_{i1}$, GST-Gα$_{i2}$, and GST-Gα$_{i3}$ and His-CalnucΔN to investigate whether Calnuc binds to other Gα$_i$ subunits. We used CalnucΔN instead of full-length Calnuc because initial experiments indicated that they shared virtually identical Gα$_i$ binding properties (data not shown). We found that His-CalnucΔN binds strongly to GDP-loaded GST-Gα$_{i1}$ and GST-Gα$_{i3}$ but showed significantly less binding to Gα$_{i2}$ (Fig. 4*B*). These results indicate that the binding preference of Calnuc for Gα subunits is Gα$_{i1}$ ≈ Gα$_{i3}$ > Gα$_{i2}$ ⋙ Gα$_o$ ≥ Gα$_s$.

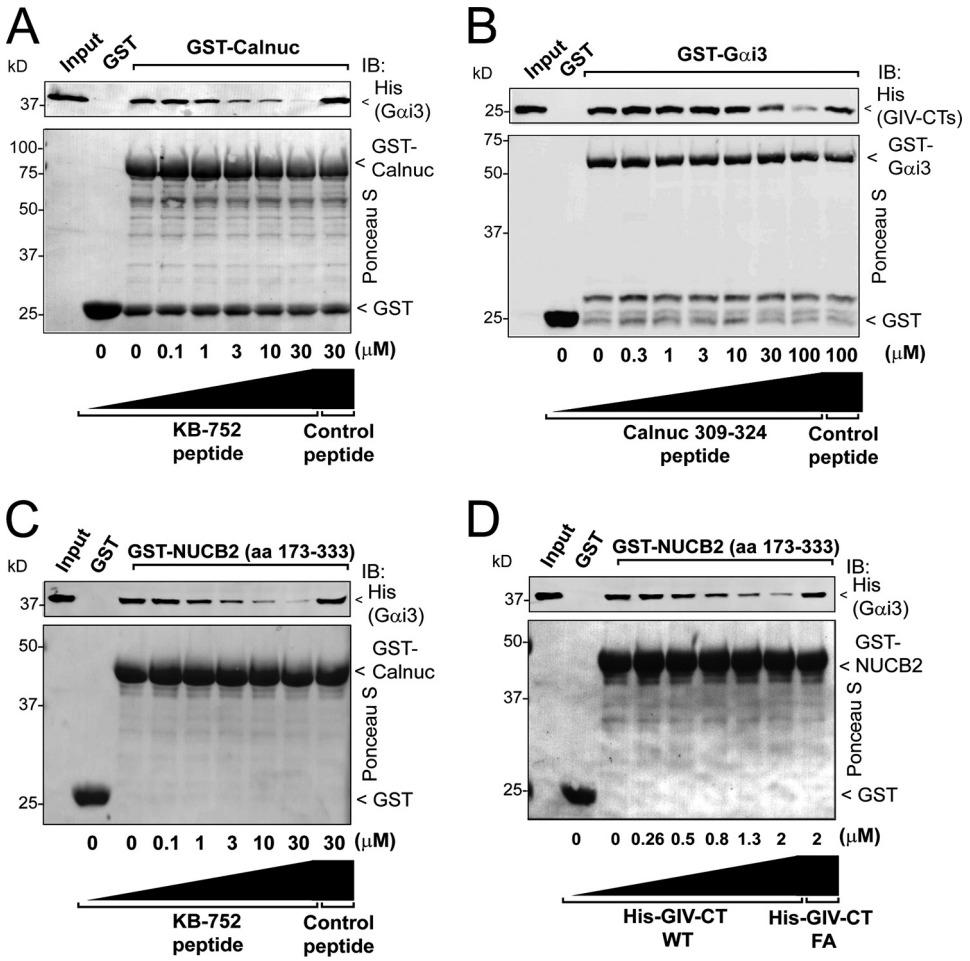


FIGURE 3. **Calnuc and NUCB2 compete with KB-752 and GIV for binding to inactive Gα$_{i3}$.** *A*, the KB-752 peptide but not a control peptide (see "Experimental Procedures") competes with GST-Calnuc for binding to His-Gα$_{i3}$·GDP. Increasing concentrations of the KB-752 peptide (0, 0.1, 1, 3, 10, and 30 μM) or control peptide (30 μM) were incubated with 20 μg (~0.9 μM) of GST-Calnuc in the presence of 6 μg (~0.5 μM) of His-Gα$_{i3}$ preloaded with GDP and analyzed as described in the legend for Fig. 2*A*. No binding of His-Gα$_{i3}$·GDP GST was detected. *Input*, 0.2 μg of His-Gα$_{i3}$·GDP. *IB*, immunoblot. *B*, a peptide corresponding to the Gα-binding motif of Calnuc 309–324 peptide, but not a control peptide, competes with His-GIV-CTs (aa 1660–1870, containing the GIV GEF motif) for binding to GST-Gα$_{i3}$·GDP. Increasing concentrations of Calnuc 309–324 peptide (0, 0.3, 1, 3, 10, 30, and 100 μM) or a control peptide (100 μM) were incubated with 3 μg (~250 nM) of GST-Gα$_{i3}$ preloaded with GDP immobilized on glutathione beads in the presence of 2 μg (~250 nM) of His-GIV-CTs and analyzed as described in the legend for Fig. 2*A*. No binding of His-GIV-CTs to GST is detected. *Input*, 0.1 μg of His-GIV-CTs. *C*, the KB-752 peptide but not a control peptide (see "Experimental Procedures") competes with GST-NUCB2 for binding to His-Gα$_{i3}$·GDP. Increasing concentrations of the KB-752 peptide (0, 0.1, 1, 3, 10, and 30 μM) or the control peptide (30 μM) were incubated with 20 μg (~1.7 μM) of GST-NUCB2 in the presence of 6 μg (~0.5 μM) of His-Gα$_{i3}$ preloaded with GDP and analyzed as described in the legend for Fig. 2*A*. No binding of His-Gα$_{i3}$·GDP to GST is detected. *Input*, 0.2 μg of His-Gα$_{i3}$·GDP. *D*, His-GIV-CTs WT but not the Gα$_i$ binding-deficient His-GIV-CTs F1685A (*FA*) (14) competes with GST-NUCB2 for binding to His-Gα$_{i3}$·GDP. Increasing concentrations of His-GIV-CTs WT (~0, 0.26, 0.5, 0.8, 1.3, and 2 μM) or His-GIV-CTs F1685A (2 μM) were incubated with 20 μg (~1.7 μM) of GST-NUCB2 in the presence of 5 μg (~0.4 μM) of His-Gα$_{i3}$ preloaded with GDP and analyzed as described in the legend for Fig. 2*A*. No binding of His-Gα$_{i3}$·GDP to GST was detected. *Input*, 0.15 μg of His-Gα$_{i3}$·GDP.

*Lys-248 in Gα$_{i3}$ Determines the Preferential Binding of Calnuc to Gα$_{i3}$ versus Gα$_o$*—Recently we found that a single residue differing between the Gα$_i$ and Gα$_o$ subunits, *i.e.* Trp-258 in Gα$_{i3}$ and Phe-259 in Gα$_o$ (Fig. 5*A*), accounts for the preferential binding of GIV to Gα$_i$ *versus* Gα$_o$ (29). To determine whether this is the case for Calnuc, we investigated the effect of mutating Trp-258 in Gα$_{i3}$ and Phe-259 in Gα$_o$ on the binding of these G proteins to Calnuc. GST-Calnuc bound robustly to purified wild-type His-Gα$_{i3}$ but not to purified wild-type His-Gα$_o$ (Fig. 5*B*); this striking preference remained unchanged when Trp-258 in Gα$_{i3}$ was mutated to Phe or when Phe-259 in Gα$_o$ was mutated to Trp (Fig. 5*B*). This indicates that Trp-258 in Gα$_i$ is not responsible for the preferential binding of Calnuc to Gα$_i$ *versus* Gα$_o$.

We reasoned that Lys-248 in Gα$_i$ could be responsible for the preferential binding to Gα$_i$ *versus* Gα$_o$ because it is the only amino acid that is not conserved between the two Gα subunits in the Calnuc binding site (Fig. 5*A*), *i.e.* the α3/SwII cleft (Fig. 3). Mutation of Lys-248 in GST-Gα$_{i3}$ to Met, the corresponding residue in Gα$_o$, dramatically decreased His-CalnucΔN binding (Fig. 5*C*). Importantly, GST-Gα$_{i3}$ K248M did bind to GIV, AGS3 (activator of G protein signaling 3), and Gβγ (Ref. 29 and data not shown), indicating that this mutation specifically affects Calnuc binding. Conversely, when Met-249 in His-Gα$_o$ was mutated to Lys, it enhanced its binding to GST-Calnuc compared with wild-type His-Gα$_o$ (Fig. 5*D*). Furthermore, structural analysis (supplemental Fig. S2*A*) revealed that the positively charged Lys-248 of Gα$_{i3}$ might establish an electrostatic interaction with negatively charged Glu-314 of Calnuc. We hypothesized that inverting the charge of the Gα$_{i3}$ Lys-248 alone would impair the Gα$_{i3}$-Calnuc interaction by electrostatic repulsion of the Calnuc Glu-314 but that inverting the

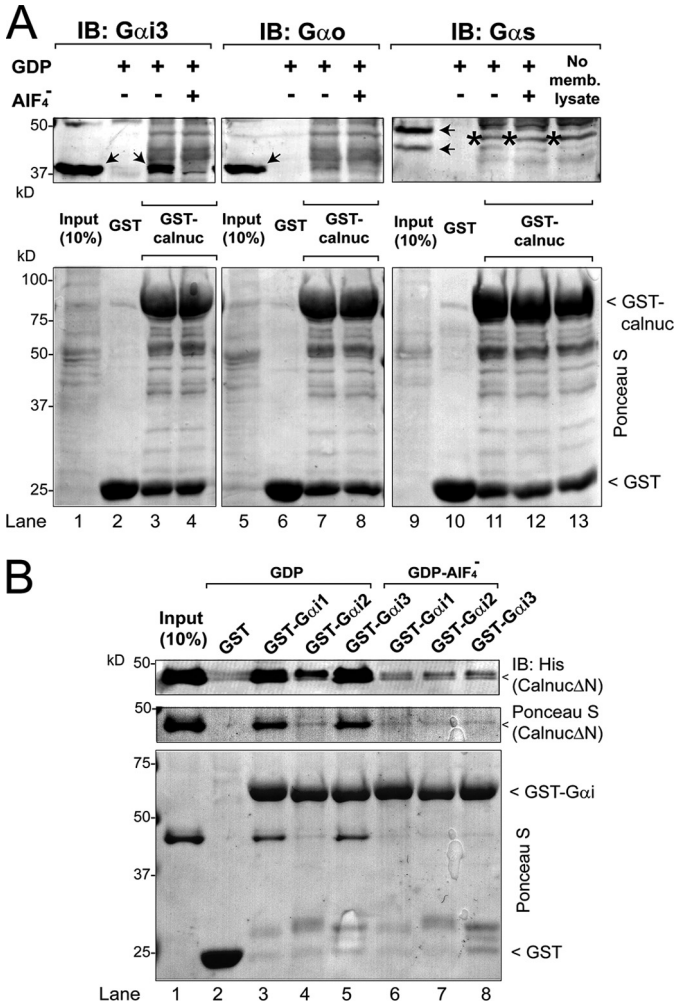


FIGURE 4. **Calnuc binds to different G$\alpha_i$ subunits but not to G$\alpha_o$ or G$\alpha_s$.** *A*, *Upper panel*, GST-Calnuc binds G$\alpha_{i3}$ (*lane 3*) but not G$\alpha_o$ (*lane 7*) or G$\alpha_s$ (*lane 11*) from rat brain membrane lysates in the presence of GDP but not GDP·AlF$_4^-$ (*lanes 4*, *8*, and *12*). Solubilized proteins from 750 $\mu$g of rat brain membranes were incubated with ~20 $\mu$g of purified GST (*lanes 2*, *6*, and *10*) or GST-Calnuc (*lanes 3*, *4*, *7*, *8*, *11*, *12*, and *13*) immobilized on glutathione beads in the presence of GDP (30 $\mu$M; *lanes 2*, *3*, *6*, *7*, *10*, and *11*) or GDP and AlF$_4^-$ (AlCl$_3$, 30 $\mu$M; NaF, 10 mM; *lanes 4*, *8*, and *12*). An additional control without rat brain membrane lysate was performed to validate G$\alpha_s$ antibody specificity (*lane 13*). *Input* (*lanes 1*, *5*, and *9*), 10% of the membrane lysate. No binding of G$\alpha_{i3}$, G$\alpha_o$, or G$\alpha_s$ to the negative control GST was detected (*lanes 2*, *6*, and *10*). The *arrows* (*lanes 1*, *3*, *5*, and *9*) denote the specific bands corresponding to the different Gα subunits (including the long and short splice forms of G$\alpha_s$, *lane 9*), and the *star* (*lanes 11*, *12*, and *13*) denotes a nonspecific band recognized by the G$\alpha_s$ antibody. *IB*, immunoblot. *Lower panel*, equal loading of GST proteins was confirmed by Ponceau S staining. *B*, His-CalnucΔN binds to GST-G$\alpha_{i1}$·GDP (*lane 3*) and GST-G$\alpha_{i3}$·GDP (*lane 5*) to a greater extent (~20-fold) than to GST-G$\alpha_{i2}$·GDP (*lane 4*) and binds only marginally to either of the G$\alpha_i$ subunits preloaded with GDP·AlF$_4^-$ (*lanes 6*, *7*, and *8*) or GST (*lane 2*). 10 $\mu$g of His-CalnucΔN was incubated with 15 $\mu$g of GST (*lane 2*), GST-G$\alpha_{i1}$ (*lanes 3* and *6*), GST-G$\alpha_{i2}$ (*lanes 4* and *7*), or GST-G$\alpha_{i3}$ (*lanes 5* and *8*) preloaded with GDP (*lanes 2–5*) or GDP·AlF$_4^-$ (*lanes 6–8*), immobilized on glutathione beads, and analyzed as described for Fig. 2*A*. *Input* (*lane 1*), 1 $\mu$g of His-CalnucΔN.

charges of these two residues simultaneously would restore the interaction by establishing an electrostatic attraction analogous to that found in the native situation. In fact, inversion of the charge of the G$\alpha_{i3}$ Lys-248 by mutation to Glu abolished G$\alpha_{i3}$ binding to wild-type Calnuc, and binding was restored if the charge of Calnuc Glu-314 was simultaneously inverted by mutation to Lys (supplemental Fig. S2*B*), suggesting that the electrostatic interaction between G$\alpha_{i3}$ aa 248 and Calnuc aa 314 stabilizes G$\alpha_{i3}$-Calnuc binding. These results demonstrate that although GIV and Calnuc have an overlapping binding site on Gα subunits, *i.e.* the α3/SwII cleft, and display preference for G$\alpha_i$ *versus* G$\alpha_o$, the critical residues in the Gα subunit that determine binding specificity are different.

*Identification of Residues in Calnuc Required for Binding and Regulating G$\alpha_i$*—Calnuc, NUCB2, GIV and GIV-related peptides share hydrophobic residues in positions 3, 6 and 7 of the consensus sequence depicted in Fig. 1*A*. In the structure of the KB-752·G$\alpha_{i1}$ complex these residues are packed against the hydrophobic cleft formed by the α3 helix and switch II to stabilize the interaction (Ref. 15 and Fig. 1*B*). We reasoned that residues in the same position might also be required for Calnuc and NUCB2 to bind G$\alpha_{i3}$. We found that mutation of each of the corresponding residues in Calnuc, *i.e.* Leu-313, Phe-316, and Leu-317 to Ala dramatically reduced His-G$\alpha_{i3}$ binding to GST-Calnuc (Fig. 6*A*). The double mutant L313A/L317A decreased the interaction even further than the single mutations (Fig. 6*A*, see *high exposure* blot). Similar findings were obtained for NUCB2 (Fig. 6*B*), indicating that these hydrophobic residues are required for both Calnuc and NUCB2 to interact with G$\alpha_{i3}$. In addition, mutation of G$\alpha_{i3}$ Trp-211 or Phe-215 in the predicted binding site for Calnuc (supplemental Fig. S3*A*) also disrupted the interaction (supplemental Fig. S3*B*), suggesting that they mediate a hydrophobic interaction with the Calnuc Leu-313, Phe-316, and Leu-317. These results indicate that the interaction of Calnuc and NUCB2 with G$\alpha_{i3}$ requires the hydrophobic residues found in their conserved motif shared with GIV and GIV-related peptides.

We next investigated the effect of Calnuc and NUCB2 on G protein activation. For this we measured the steady-state GTPase activity of His-G$\alpha_{i3}$ (which depends directly on the rate of nucleotide exchange (29, 35)) in the presence of wild-type His-CalnucΔN or His-CalnucΔN L313A/L317A, which has dramatically impaired binding to G$\alpha_{i3}$ (Fig. 6*A*) (negative control). His-CalnucΔN was used instead of full-length His-Calnuc because the protein concentrations used in these experiments were achievable only for the truncated protein, which expresses at higher yields in bacteria (see "Experimental Procedures"). Wild-type CalnucΔN but not CalnucΔN L313A/L317A increased the rate of steady-state GTP hydrolysis (Fig. 7*A*). Similarly, wild-type GST-NUCB2 but not its binding-deficient mutant, L315A/L319A, also increased the steady-state GTPase activity of G$\alpha_{i3}$ (Fig. 7*B*). Other mutants of the Gα-binding motif such as Calnuc F316A and NUCB2 F318A also impaired G$\alpha_{i3}$ activation when compared with their respective wild-type controls (supplemental Fig. S4), suggesting that Calnuc and NUCB2 are GEFs for G$\alpha_{i3}$ and that they work via their conserved Gα-binding motif. Wild-type CalnucΔN and NUCB2 increased the GTPase activity of His-G$\alpha_{i3}$ 1.74- ± 0.18-fold ($n = 6$) and 1.76- ± 0.13-fold ($n = 3$), respectively, at the maximal concentration tested (Fig. 7*C*). The $EC_{50}$ values were 7.3 ± 1.0 $\mu$M and 4.0 ± 1.0 $\mu$M (Fig. 7*C*), which are in good agreement with their respective $K_d$ values for G$\alpha_{i3}$ binding (Fig. 2*C*). To further validate the role of Calnuc as a GEF, we performed GTPγS binding experiments, which are a direct measure of GDP for GTP exchange activity. Incubation of His-G$\alpha_{i3}$ in the presence of CalnucΔN increased the initial rate of GTPγS bind-

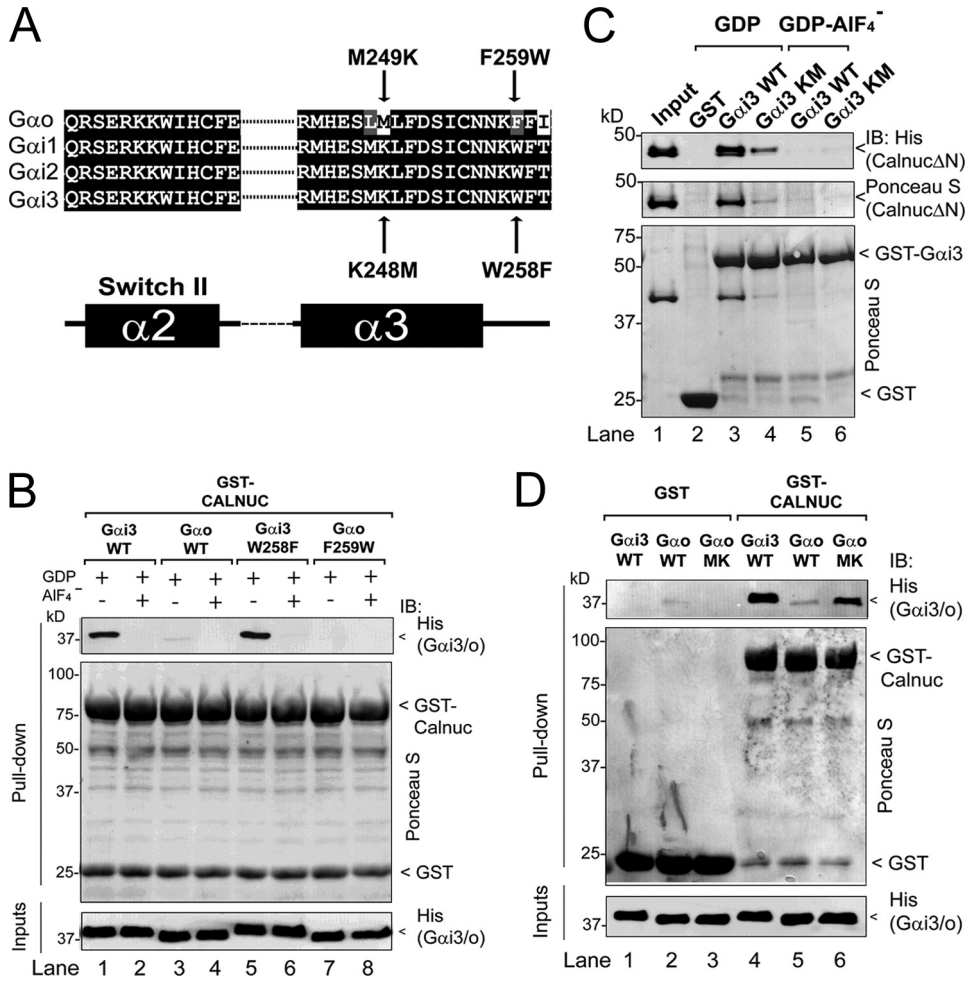


FIGURE 5. **Lys-248 but not Trp-258 is responsible for preferential binding of Calnuc to Gα$_{i3}$ *versus* Gα$_o$.** *A*, sequence alignment of Gα$_o$, Gα$_{i1}$, Gα$_{i2}$, and Gα$_{i3}$ indicating the Gα$_{i3}$ and Gα$_o$ mutants studied. Rat Gα$_o$, Gα$_{i1}$, Gα$_{i2}$, and Gα$_{i3}$ sequences corresponding to the SwII and the α3 helix were obtained from the NCBI database and aligned using ClustalW. Conserved identical residues are shaded in *black* and similar residues in *gray*. The secondary structure elements (α = α-helix, β = β-sheet) indicated below the alignment are named according to their crystal structures. Residues within this region that are conserved among Gα$_{i1}$, Gα$_{i2}$, and Gα$_{i3}$ but are different in Gα$_o$ were mutated in Gα$_{i3}$ to the corresponding residues in Gα$_o$ (indicated below with *arrows*) or in Gα$_o$ to the corresponding residues in Gα$_{i3}$ (indicated above with *arrows*). *B*, wild-type His-Gα$_{i3}$·GDP (*lane 1*) and His-Gα$_{i3}$·GDP W258F (*lane 5*) but not wild-type His-Gα$_o$·GDP (*lane 3*) or His-Gα$_o$·GDP F259W (*lane 7*) bind to GST-Calnuc. No binding of any of the Gα subunits loaded with GDP·AlF$_4^-$ to GST-Calnuc was detected (*lanes 2*, *4*, *6*, and *8*). 6 μg of His-Gα$_{i3}$ (*lanes 1* and *2*), His-Gα$_o$ (*lanes 3* and *4*), His-Gα$_{i3}$ W258F (*lanes 5* and *6*), or His-Gα$_o$ F259W (*lanes 7* and *8*) preloaded with GDP (*lanes 1*, *3*, *5*, and *7*) or GDP and AlF$_4^-$ (*lanes 2*, *4*, *6*, and *8*) was incubated with ~20 μg of purified GST-Calnuc immobilized on glutathione beads and analyzed as described in the legend for Fig. 2*A*. *C*, His-CalnucΔN binding to GST-Gα$_{i3}$ K248M·GDP (Gα$_{i3}$ $K_m$ (*lane 4*)) is reduced ~80% compared with wild-type GST-Gα$_{i3}$·GDP (Gα$_{i3}$ WT, *lane 3*). No binding of His-CalnucΔN to GST (*lane 2*) or GDP·AlF$_4^-$-loaded Gα$_{i3}$ (*lanes 5* and *6*) is detected. 10 μg of His-CalnucΔN was incubated with purified GST (*lane 2*), wild-type GST-Gα$_{i3}$ (*lanes 3* and *5*), or GST-Gα$_{i3}$ K248M (*lanes 4* and *6*) preloaded with GDP (*lanes 2–4*) or GDP·AlF$_4^-$ (*lanes 5* and *6*) immobilized on glutathione beads and analyzed as described in the legend for Fig. 2*A*. *Input* (*lane 1*), 1 μg of His-CalnucΔN. *IB*, immunoblot. *D*, wild-type His-Gα$_{i3}$·GDP (Gα$_{i3}$ WT (*lane 4*)) and His-Gα$_o$ M249K·GDP (Gα$_o$ MK (*lane 6*)) but not wild-type His-Gα$_o$ (Gα$_o$ WT (*lane 5*)) bind to GST-Calnuc. No binding of any of the Gα subunits to GST is detected (*lanes 1–3*). 6 μg of each His-Gα subunit preloaded with GDP was incubated with ~20 μg of purified GST (*lanes 1–3*) or GST-Calnuc (*lanes 4–6*) immobilized on glutathione beads and analyzed as in the legend for Fig. 2*A*.

ing 1.70- ± 0.10-fold ($n = 4$) compared with the G protein alone (Fig. 7*D*). Taken together, these results indicate that the Gα$_i$-binding motif in Calnuc and NUCB2 has GEF activity toward Gα$_{i3}$.

*Effect of Calcium Binding to Calnuc and NUCB2 on Their Interaction with Gα$_{i3}$*—The domain of Calnuc containing both EF-hands is known to be disorganized in the absence of $Ca^{2+}$ and to adopt a globular conformation upon binding of the divalent cation (34). Analysis of the structure of calcium-bound Calnuc revealed that the residues that interact with Gα$_{i3}$, *i.e.* Leu-313, Phe-316, and Leu-317 (Fig. 6*A*), are also utilized to make an intramolecular contact in the calcium-bound conformation (Fig. 8*A*), suggesting that Calnuc would not be able to interact with Gα$_{i3}$ upon binding of $Ca^{2+}$. We found this to be the case, because neither Calnuc nor NUCB2 bound Gα$_{i3}$ in the presence of excess $CaCl_2$ (Fig. 8, *B* and *C*). No difference was observed when the experiment was performed in the presence of excess $MgCl_2$ or LiCl (data not shown), indicating that the observed effect is specific for $Ca^{2+}$. We also investigated the effect of $Ca^{2+}$ on the GEF activity of Calnuc and found that increasing concentrations of $Ca^{2+}$ inhibited the increase in GTPγS binding to Gα$_{i3}$ promoted by Calnuc with an $IC_{50}$ of 1.2 ± 0.12 μM ($n = 3$) (Fig. 8*D*), a value similar to the previously reported $K_d$ of Calnuc for $Ca^{2+}$. Finally, we investigated the effect of elevating intracellular $Ca^{2+}$ levels on the interaction between Calnuc and Gα$_{i3}$ in cultured cells. COS-7 cells were co-transfected with Gα$_{i3}$-FLAG and a truncated Calnuc (ΔSS-Calnuc-CFP), lacking the signal sequence which is present pre-

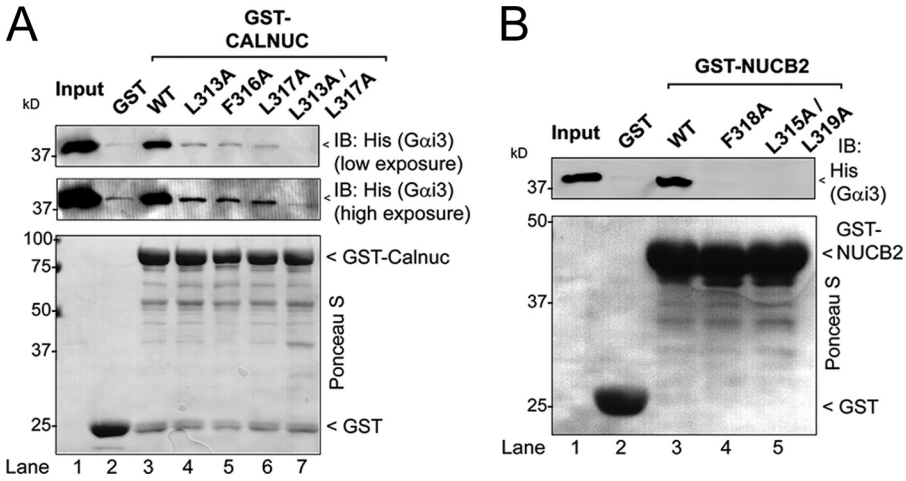


FIGURE 6. **Identification of critical residues in Calnuc required for binding Gα$_{i3}$.** *A*, His-Gα$_{i3}$·GDP binds to wild-type GST-Calnuc (*lane 3*) but not to GST-Calnuc mutants L313A (*lane 4*), F316A (*lane 5*), L317A (*lane 6*), or L313A/L317A (*lane 7*) or GST alone (*lane 2*). 6 μg of His-Gα$_{i3}$ preloaded with GDP (30 μM) was incubated with ~20 μg of purified GST (*lane 2*), wild-type GST-Calnuc (*lane 3*), or GST-Calnuc mutants L313A (*lane 4*), F316A (*lane 5*), L317A (*lane 6*), or L313A/L317A (*lane 7*) immobilized on glutathione beads and analyzed as described in the legend for Fig. 2*A*. *Input* (*lane 1*), 0.1 μg of His-Gα$_{i3}$. *IB*, immunoblot. *B*, His-Gα$_{i3}$·GDP binds to wild-type GST-NUCB2-(173–333) (*lane 3*) but not to GST-NUCB2 mutants F318A (*lane 4*) or L315A/L319A (*lane 5*) or to GST alone (*lane 2*). 6 μg of His-Gα$_{i3}$ preloaded with GDP (30 μM) was incubated with ~20 μg of purified GST (*lane 2*), wild-type GST-NUCB2 (*lane 3*), or GST-Calnuc mutants L313A (*lane 4*) or L315A/L319A (*lane 5*) immobilized on glutathione beads and analyzed as described in the legend for Fig. 2*A*. *Input* (*lane 1*), 0.1 μg of His-Gα$_{i3}$.

dominantly in the cytosol (26). Cells were stimulated with thapsigargin (which elevates the cytosolic levels of $Ca^{2+}$ by blocking the endoplasmic reticulum $Ca^{2+}$ pump) or ATP (which activates purinergic receptors at the cell surface) (22), and immunoprecipitation was carried out using anti-FLAG IgG followed by immunoblotting for Calnuc. We found that ΔSS-Calnuc-CFP co-immunoprecipitated with Gα$_{i3}$ exclusively in non-stimulated cells, but it was virtually abolished after stimulation with either thapsigargin or ATP (Fig. 8*E*). Co-immunoprecipitation of Gβγ with Gα$_{i3}$-FLAG was not affected by thapsigargin or ATP, indicating that elevation of the intracellular levels of $Ca^{2+}$ specifically affects the interaction of Gα$_{i3}$ with Calnuc but not other Gα-binding proteins. These results suggest that elevation of intracellular $Ca^{2+}$ levels can efficiently disrupt the interaction between Calnuc and Gα$_{i3}$ in living cells, corroborating our observations *in vitro*. Taken together, these data indicate that calcium binding can promote conformational changes in Calnuc (and presumably also in NUCB2) that block its interaction with Gα subunits *in vitro* and in living cells (Fig. 8*F*), subsequently inhibiting its GEF activity.

## DISCUSSION

In this work we identify a new class of G protein-binding motif with defined structural features. This motif is found in two closely related proteins, Calnuc and NUCB2, and was previously found in another unrelated protein, GIV, and in the synthetic peptides KB-752 and GSP, shown previously to have GEF activity for Gα$_i$ (15, 33). It consists of a relatively disordered N-terminal region followed by an α-helix that docks onto the α3/SwII cleft of the Gα$_i$ subunits only in the inactive conformation to enable GEF activity *in vitro*. We named this signature sequence the GBA motif (for Gα-binding and -activating motif). We propose that the conserved GBA motif found in native proteins is a signature structure that defines a new family of G protein regulators with GEF activity, in the same fashion as the GoLoco/GPR motif or the RGS box define families of proteins with GDI or GTPase-activating protein activity, respectively. An important observation is that the GBA motif in Calnuc is evolutionarily conserved across species from sponges to man (supplemental Fig. S1), and the *Caenorhabditis elegans* orthologues of Calnuc and the Gα subunits have been shown to interact (36), suggesting that its function as a Gα-binding motif is also evolutionarily conserved. This evolutionary conservation suggests a selection imposed by a crucial biological function associated with the interaction with Gα$_i$. It is interesting that a similar consensus motif was found in two synthetic peptides, KB-752 and GSP, which were identified by two different *in vitro* approaches, phage display of random sequence peptides (15) and iterative optimization of *in vitro* mRNA-translated peptides (33). In both cases the selection is determined solely by the chemical properties of the peptides and not their biological function. These observations suggest that the sequences found *in vivo* in the GBA motif of Calnuc, NUCB2, and GIV have highly optimized chemical properties for Gα$_i$ binding.

Based on the sequences of Calnuc, NUCB2, and GIV in different species (supplemental Fig. S1 and Ref. 14) and related synthetic peptides (15, 33), we propose that the GBA motif can be defined by a conserved core sequence of seven amino acids (Fig. 1*A*), Ψ-[S/T]-[Φ/Ψ]-*X*-[D/E]-F-Ψ, in which Ψ are aliphatic residues and Φ are aromatic residues. Residues in positions 3, 6, and 7 in this consensus motif, *i.e.* Leu-313, Phe-316, and Leu-317 in Calnuc, correspond to hydrophobic residues aligned on one side of the α-helical part of the motif, which are used to stabilize the interaction with Gα$_i$ by packing against the α3/SwII hydrophobic cleft. Residues in positions 2 and 5 form a hydrogen bond in the structures of KB-752 and Calnuc, which is required for the motif to adopt its helical conformation. This design for molecular coupling resembles that observed for other signaling interfaces. For example, A-kinase-anchoring proteins (AKAPs) are characterized by a signature motif that

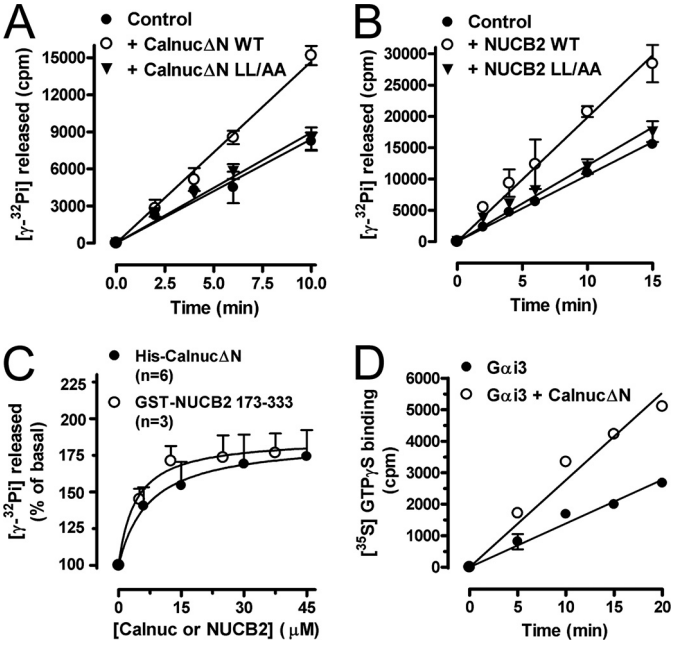


FIGURE 7. **Calnuc and NUCB2 activate Gα$_{i3}$.** *A*, His-CalnucΔN WT but not the L313A/L317A (*LL/AA*) mutant increases the steady-state GTPase activity of His-Gα$_{i3}$. The steady-state GTPase activity of purified His-Gα$_{i3}$ (50 nM) was determined in the absence (*closed circles*) or presence of 60 μM purified wild-type His-CalnucΔN (*open circles*) or His-CalnucΔN L315A/L319A mutant (*inverted triangles*) by quantifying the amount of [γ-$^{32}$P]GTP (0.5 μM, ~50 cpm/fmol) hydrolyzed at the indicated time points. Results are shown as mean ± S.D. of one representative experiment of three performed in duplicate. *B*, WT GST-NUCB2-(173–333) but not the L315A/L319A mutant increases the steady-state GTPase activity of His-Gα$_{i3}$. The steady-state GTPase activity of purified His-Gα$_{i3}$ (100 nM) was determined exactly as described in *A* except that 50 μM NUCB2 was used. *C*, dose-dependent activation of His-Gα$_{i3}$ by His-CalnucΔN and GST-NUCB2. The steady-state GTPase activity of purified His-Gα$_{i3}$ was determined in the presence of the indicated amounts of purified wild-type His-CalnucΔN (*closed circles*) or GST-NUCB2 (*open circles*) by quantification of the amount of [γ-$^{32}$P]GTP (0.5 μM, ~50 cpm/fmol) hydrolyzed in 10 min. Data expressed as percent of GTP hydrolyzed by the G protein alone (0 μM) were fitted to a nonlinear, one-site hyperbola (*solid line*) using Prism 4.0. Results are shown as mean ± S.E. of the indicated number of experiments (*n*). *D*, His-CalnucΔN increases the rate of GTPγS binding of His-Gα$_{i3}$. Nucleotide exchange activity of purified His-Gα$_{i3}$ (50 nM) was determined in the absence (*closed circles*) or presence of 25 μM purified wild-type His-CalnucΔN (*open circles*) by quantification of the amount of [$^{35}$S]GTPγS (0.5 μM, ~50 cpm/fmol) bound at the indicated time points. No significant binding of GTPγS binding was detected in the absence of His-Gα$_{i3}$ or the presence of His-CalnucΔN alone (not shown). Results are shown as mean ± S.D. of one representative experiment of four performed in duplicate.

forms an aliphatic helix that docks onto a hydrophobic pocket on the regulatory subunit of cAMP-dependent protein kinase (PKA) (37), and the N-terminal region of the GoLoco/GPR motif, also binds to the α3/SwII hydrophobic cleft of Gα$_i$ subunits via an aliphatic helix (10).

Our results also provide the structural basis for the regulation of Calnuc and NUCB2 binding to and activation of Gα$_i$ subunits by calcium. Calnuc is the major calcium-binding protein in the lumen of Golgi cisternae, where it regulates the intracellular calcium stores (21, 22). On the other hand, there is a cytosolic pool of Calnuc that interacts directly with Gα$_{i3}$ (26). NUCB2 has been described as sharing a similar subcellular distribution (20). The regulation of the Calnuc/NUCB2-Gα$_i$ interaction by $Ca^{2+}$ described in this work is not surprising considering that the Gα-binding motif on Calnuc overlaps with the EF-hands responsible for calcium binding. Our finding that Gα$_i$ binding to Calnuc and NUCB2 is impaired by calcium binding is compatible with previous observations by NMR indicating that when calcium-bound, the Calnuc EF-hands fold into a globular domain that hides the Gα$_i$-binding residues, whereas in the absence of calcium this domain is disordered and probably exposes the Gα$_i$-binding motif (Fig. 8*F*). Thus, we propose that the conformational changes in Calnuc and NUCB2 that occur upon $Ca^{2+}$ binding regulate their interaction with the G protein and its subsequent activation. This mode of regulation by $Ca^{2+}$ is consistent with our results presented here indicating that Calnuc and Gα$_{i3}$ interact in the cytosol of cells under resting conditions (in accord with our own previous observation using FRET and live cell microscopy (26)) but not upon stimulation with thapsigargin or ATP (Fig. 8*E*). This is probably because in resting conditions the cytosolic concentration of free $Ca^{2+}$ (50–100 nM) is significantly lower than the $K_d$ value of Calnuc for $Ca^{2+}$ binding (~7 μM, (22)), thereby allowing the interaction of calcium-free Calnuc with Gα$_{i3}$, whereas upon stimulation with thapsigargin or ATP the intracellular levels of $Ca^{2+}$ are increased and calcium-bound Calnuc cannot interact with Gα$_{i3}$. It will be important in the future to ask whether the regulation of the Calnuc-Gα$_{i3}$ interaction by $Ca^{2+}$ might influence the interplay between G protein- and calcium-dependent signaling, two major signaling events that regulate a multitude of cellular functions.

Our data also unveiled the structural basis for the state-dependent binding of Calnuc and NUCB2 to Gα$_i$ subunits. Based on the structures of Gα$_{i1}$ and other Gα subunits bound to GTPγS and GDP- $AlF_4^-$ (38, 39), the hydrophobic cleft circumscribed by the α3 helix and the switch II is occluded when the G protein adopts the active conformation, thereby hindering its interaction with Calnuc and NUCB2 by steric clashes. From this we concluded that conformational changes of Gα$_{i3}$ upon activation determine its interaction with Calnuc and NUCB2. We previously reported that Calnuc binds to a site different from the α3/SwII cleft (*i.e.* the α5 helix) of Gα$_{i3}$ by using C-terminal truncations of the G protein (25). Although we cannot rule out the presence of two binding sites for Calnuc on Gα$_i$ subunits, one likely explanation for the previous results is that truncation of the Gα$_i$ C terminus promotes constitutive activation of the G protein (40) which in light of the data presented here would abolish its interaction with Calnuc and NUCB2.

The studies presented here also provide insights into the specific features of the Calnuc-Gα subunit interface and its differences from another GBA motif-containing protein, *i.e.* GIV. Both Calnuc and GIV bind preferentially to Gα$_i$ subunits over Gα$_o$ or Gα$_s$, but Calnuc shows preference for Gα$_{i1}$ and Gα$_{i3}$ over Gα$_{i2}$, whereas GIV binds equally to Gα$_{i1}$, Gα$_{i2}$, and Gα$_{i3}$ *in vitro* (14). The basis for the preference of Calnuc for Gα$_{i1}$ and Gα$_{i3}$ over Gα$_{i2}$ is still unclear, because all Gα$_i$ subunits have identical residues in the switch II and the α3 helix (Fig. 5*A*), which based on our results presented here is a major binding site for Calnuc on the G protein. It is possible that other residues of the G protein outside of this major binding surface, *i.e.* the α3/SwII cleft, may also determine the specificity of binding by making additional contacts, as reported for other G protein regulators with preference for Gα$_{i1}$ and Gα$_{i3}$ over Gα$_{i2}$ such as

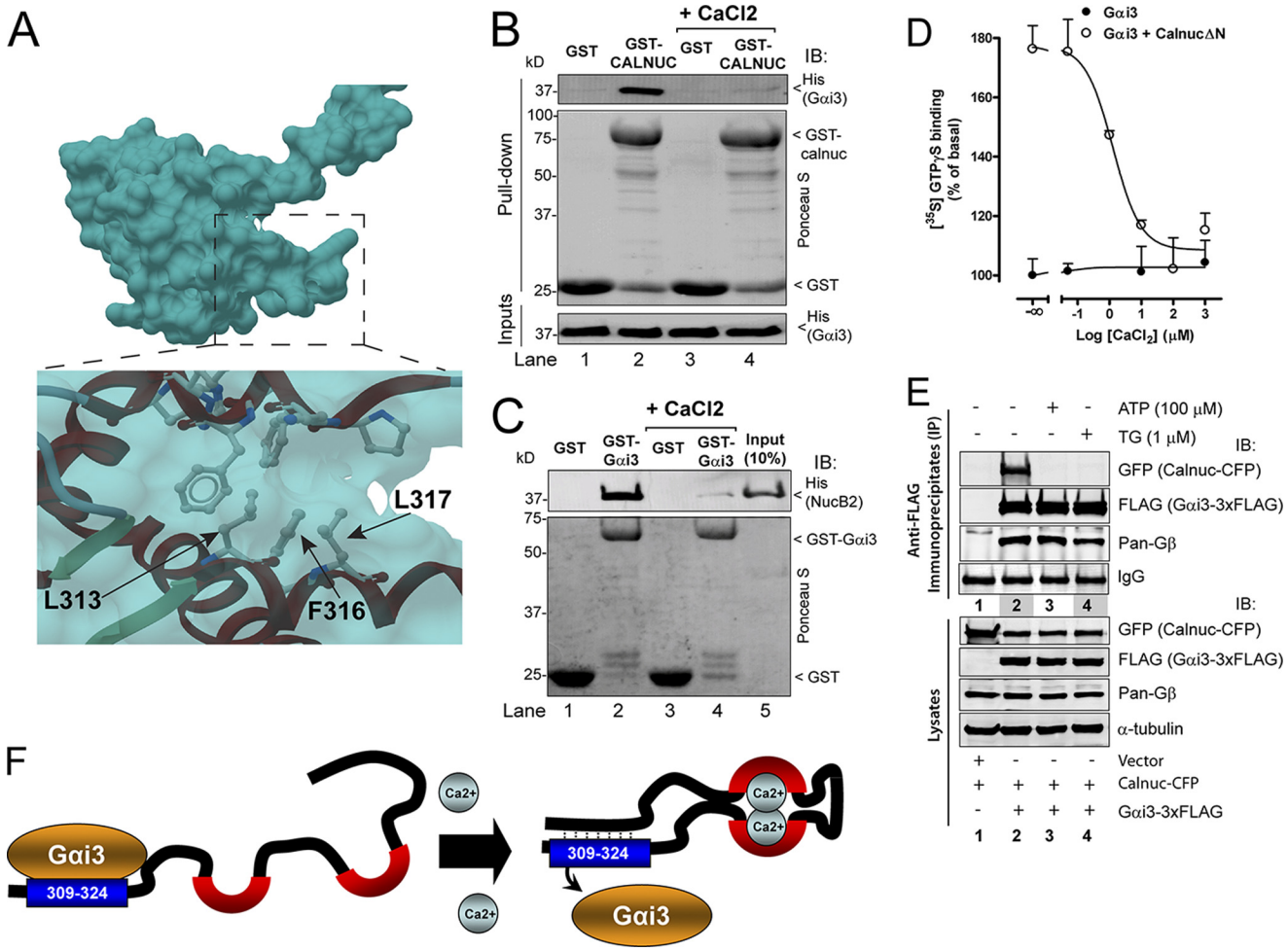


FIGURE 8. **Effect of $Ca^{2+}$ on Calnuc and NUCB2 binding to G$\alpha_{i3}$.** *A*, structural view of the G$\alpha_i$-binding motif of Calnuc in the calcium-bound conformation. The coordinates of the NMR-resolved structure of Calnuc were extracted from the Protein Data Bank (ID code: 1SNL) and visualized using ICM-Browser-Pro. Residues of the G$\alpha_i$-binding motif of Calnuc required for the interaction with G$\alpha_{i3}$ (Fig. 6) are not solvent-exposed in the calcium-bound conformation of Calnuc because they were utilized to make an intramolecular contact. *B*, His-G$\alpha_{i3}$ binding to GST-Calnuc is virtually abolished in the presence of $CaCl_2$. 6 μg of His-G$\alpha_{i3}$ preloaded with GDP (30 μM) was incubated with ~20 μg of purified GST (*lanes 1* and *3*) or GST-Calnuc (*lanes 2* and *4*) immobilized on glutathione beads in the presence (*lanes 3* and *4*) or absence (*lanes 1* and *2*) of 8 mM $CaCl_2$ (~3 mM free $Ca^{2+}$). Subsequent steps were performed as described in the legend for Fig. 2*A*. *C*, binding of GST-G$\alpha_{i3}$ to His-NUCB2 is virtually abolished in the presence of $CaCl_2$. 10 μg of His-NUCB2 was incubated with purified GST (*lanes 1* and *3*) or GST-G$\alpha_{i3}$ (*lanes 2* and *4*) immobilized on glutathione beads in the presence (*lanes 3* and *4*) or absence (*lanes 1* and *2*) of 8 mM $CaCl_2$ (~3 mM free $Ca^{2+}$). Subsequent steps were performed as described in the legend for Fig. 2*B*. *Input* (*lane 5*), 1 μg of His-NUCB2. *D*, activation of His-G$\alpha_{i3}$ by His-CalnucΔN is inhibited by $CaCl_2$ in a dose-dependent manner. Nucleotide exchange activity of purified His-G$\alpha_{i3}$ (50 nM) at the indicated concentrations of $CaCl_2$ was determined in the absence (*closed circles*) or presence of 25 μM purified wild-type His-CalnucΔN (*open circles*) by quantification of the amount of [$^{35}$S] GTPγS (0.5 μM, ~50 cpm/fmol) bound at 20 min. Results are shown as mean ± S.D. of one representative of three independent experiments performed in duplicate. $CaCl_2$ does not affect the basal activity of G$\alpha_{i3}$ alone (*closed circles*). *E*, stimulation of COS-7 cells with thapsigargin or ATP inhibits the interaction of Calnuc with G$\alpha_{i3}$. *Upper panels*, co-immunoprecipitation of ΔSS-Calnuc-CFP but not Gβγ with G$\alpha_{i3}$-FLAG is dramatically reduced after stimulation with thapsigargin (*TG*) (*lane 3*) or ATP (*lane 4*) compared with unstimulated cells (*lane 2*). No ΔSS-Calnuc-CFP or Gβγ was detected in FLAG immunoprecipitates of cells transfected with vector control (*lane 1*). COS-7 cells were transfected with empty vector (*lane 1*) or plasmids encoding G$\alpha_{i3}$-FLAG and ΔSS-Calnuc-CFP (*lanes 2*, *3*, and *4*), stimulated with thapsigargin (*lane 3*) or ATP (*lane 4*) and immunoprecipitated (*IP*) as described under "Experimental Procedures." Immunoprecipitation was followed by immunoblotting (*IB*) for FLAG (G$\alpha_{i3}$), GFP (ΔSS-Calnuc-CFP), and Gβ. Equal IgG loading was confirmed by Ponceau S staining. *Lower panels*, aliquots of the lysates (10%) were analyzed by immunoblotting to confirm equal loading of G$\alpha_{i3}$, Calnuc, Gβ, and α-tubulin. *F*, schematic illustration of how $Ca^{2+}$ binding to Calnuc mediates a molecular rearrangement that prevents G$\alpha_{i3}$ binding. *Left*, in the absence of $Ca^{2+}$, the Calnuc calcium-binding domain (*black line* with *red semicircles*) is disordered (34) allowing the exposure of the G$\alpha_i$-binding motif (aa 309–324 (*blue box*)). *Right*, in the presence of $Ca^{2+}$, Calnuc undergoes a conformational change such that residues in the G$\alpha_i$-binding motif (*blue box*) make an intramolecular interaction (*dotted lines*) and binding to G$\alpha_{i3}$ is hindered because the G$\alpha_i$-binding motif is not exposed. Presumably the same occurs for the NUCB2 G$\alpha_i$-binding motif (aa 311–326) upon calcium binding.

GAIP/RGS19 (41), RGS14 (42, 43), and RGS12 (44). As in the case of GIV (29), binding of Calnuc to G$\alpha_o$ is marginal compared with binding to G$\alpha_{i3}$. We provide evidence here that the preferential binding of Calnuc to G$\alpha_i$ over G$\alpha_o$ is determined by Lys-248, located in the middle of the α3 helix of the G protein, but not by Trp-258, located in the α3/β5 loop, which we have previously shown to be responsible for the preferential binding of GIV to G$\alpha_i$ *versus* G$\alpha_o$ (29). Based on the results presented here on Calnuc (Figs. 5 and 6 and supplemental Figs. S2 and S3) and our own published (14, 29) and unpublished data on GIV, we propose that conserved hydrophobic residues in Calnuc and the GIV GBA motif are required to dock onto a common spot of G$\alpha_{i3}$, *i.e.* the α3/SwII hydrophobic cleft, whereas nonconserved residues establish a set of contacts with the G protein that is different for Calnuc or GIV (see details in supplemental Fig. S5). These variations in the common theme highlight the uniqueness of the interfaces formed between different GBA motif-containing proteins and the G protein, which may be relevant for achieving spec-

ificity in the pharmacological targeting of these interfaces for therapeutic purposes, as proposed for GIV (14, 29).

Our results suggest a role for Calnuc and NUCB2 as regulators of G protein activity. The affinity of Calnuc and NUCB2 for $G\alpha_{i3}$ ($K_d$ ~4 and ~1 μM, respectively) is lower than that of GIV ($K_d$ ~300 nM, data not shown) but similar to the GEF peptide KB-752 ($K_d$ ~4 μM (15)) and other G protein regulators such as the GDI proteins LGN ($K_d$ ~6 μM (45)) and G18/AGS4 ($K_d$ ~2.5 μM (46)). Like GIV and related synthetic peptides, Calnuc and NUCB2 possess GEF activity *in vitro*, indicating that this is a common feature associated with the conserved GBA motif. While this manuscript was in preparation, Kapoor *et al.* (47) reported that Calnuc possesses GDI activity toward $G\alpha_{i1}$. Although the reason for the discrepancy between their work and ours is not clear, one possible explanation is the different experimental conditions used; specifically, Kapoor *et al.* (47) used ~200–400-fold higher concentrations of G protein and nucleotide in their G protein activity assays than those used here and in most previous studies of this type (6, 7, 10, 14, 15, 29, 33, 40, 48) which might affect the enzymatic properties of the reaction studied. In addition, some of the evidence presented by Kapoor *et al.* (47) is based on spectroscopic studies with fluorescent nucleotide analogs, and this type of analysis has been reported to generate artifactual readouts (48) for peptides such as Calnuc that bind to the α3/SwII cleft (Fig. 3). By using the $G\alpha_i$ binding-deficient mutants L313A/L317A and F316A of Calnuc as a negative controls (Figs. 6 and S4*A*), we demonstrated that the observed increase in G protein activation can be attributed specifically to the GBA motif. The Calnuc interaction with and activation of $G\alpha_{i3}$ occurs at relatively high concentrations *in vitro*, and its GEF activity is weaker than that observed for GIV or G protein-coupled receptors. However, our previously published data demonstrate that the interaction occurs *in vivo* because cytosolic Calnuc and $G\alpha_{i3}$ bind to each other in living cells as determined by FRET and live cell imaging (26) and that Calnuc regulates the subcellular localization of $G\alpha_{i3}$ (27), suggesting a functional role for the Calnuc-$G\alpha_i$ coupling in the physiological setting. Further investigations will be required to elucidate whether $G\alpha_{i3}$ activation by Calnuc occurs *in vivo* and to determine the functional consequences of the interaction.

*Acknowledgments—We thank Xianshi Cui and Steve Dowdy for synthesizing and purifying the Calnuc-(309–324) peptide, Sekar Menon and Susan Ferro-Novick for access to the FPLC apparatus used for protein purification, and David Siderovski for kindly providing the pMCSG7 vector. We also thank Michelle Adia and Qi Zhong for valuable technical assistance.*

## REFERENCES

1. Sato, M., Blumer, J. B., Simon, V., and Lanier, S. M. (2006) *Annu. Rev. Pharmacol. Toxicol.* **46,** 151–187
2. Blumer, J. B., Smrcka, A. V., and Lanier, S. M. (2007) *Pharmacol. Ther.* **113,** 488–506
3. Siderovski, D. P., and Willard, F. S. (2005) *Int. J. Biol. Sci.* **1,** 51–66
4. De Vries, L., Zheng, B., Fischer, T., Elenko, E., and Farquhar, M. G. (2000) *Annu. Rev. Pharmacol. Toxicol.* **40,** 235–271
5. Ross, E. M., and Wilkie, T. M. (2000) *Annu. Rev. Biochem.* **69,** 795–827
6. De Vries, L., Fischer, T., Tronchère, H., Brothers, G. M., Strockbine, B., Siderovski, D. P., and Farquhar, M. G. (2000) *Proc. Natl. Acad. Sci. U.S.A.* **97,** 14364–14369
7. Peterson, Y. K., Bernard, M. L., Ma, H., Hazard, S., 3rd, Graber, S. G., and Lanier, S. M. (2000) *J. Biol. Chem.* **275,** 33193–33196
8. Tesmer, J. J., Berman, D. M., Gilman, A. G., and Sprang, S. R. (1997) *Cell* **89,** 251–261
9. Soundararajan, M., Willard, F. S., Kimple, A. J., Turnbull, A. P., Ball, L. J., Schoch, G. A., Gileadi, C., Fedorov, O. Y., Dowler, E. F., Higman, V. A., Hutsell, S. Q., Sundström, M., Doyle, D. A., and Siderovski, D. P. (2008) *Proc. Natl. Acad. Sci. U.S.A.* **105,** 6457–6462
10. Kimple, R. J., Kimple, M. E., Betts, L., Sondek, J., and Siderovski, D. P. (2002) *Nature* **416,** 878–881
11. Kimple, A. J., Yasgar, A., Hughes, M., Jadhav, A., Willard, F. S., Muller, R. E., Austin, C. P., Inglese, J., Ibeanu, G. C., Siderovski, D. P., and Simeonov, A. (2008) *Comb. Chem. High Throughput Screen.* **11,** 396–409
12. Sjogren, B., Blazer, L. L., and Neubig, R. R. (2010) *Prog. Mol. Biol. Transl. Sci.* **91,** 81–119
13. Le-Niculescu, H., Niesman, I., Fischer, T., DeVries, L., and Farquhar, M. G. (2005) *J. Biol. Chem.* **280,** 22012–22020
14. Garcia-Marcos, M., Ghosh, P., and Farquhar, M. G. (2009) *Proc. Natl. Acad. Sci. U.S.A.* **106,** 3178–3183
15. Johnston, C. A., Willard, F. S., Jezyk, M. R., Fredericks, Z., Bodor, E. T., Jones, M. B., Blaesius, R., Watts, V. J., Harden, T. K., Sondek, J., Ramer, J. K., and Siderovski, D. P. (2005) *Structure* **13,** 1069–1080
16. Garcia-Marcos, M., Jung, B. H., Ear, J., Cabrera, B., Carethers, J. M., and Ghosh, P. (2011) *FASEB J.* **22,** 590–599
17. Ghosh, P., Garcia-Marcos, M., Bornheimer, S. J., and Farquhar, M. G. (2008) *J. Cell Biol.* **182,** 381–393
18. Anai, M., Shojima, N., Katagiri, H., Ogihara, T., Sakoda, H., Onishi, Y., Ono, H., Fujishiro, M., Fukushima, Y., Horike, N., Viana, A., Kikuchi, M., Noguchi, N., Takahashi, S., Takata, K., Oka, Y., Uchijima, Y., Kurihara, H., and Asano, T. (2005) *J. Biol. Chem.* **280,** 18525–18535
19. Weng, L., Enomoto, A., Ishida-Takagishi, M., Asai, N., and Takahashi, M. (2010) *Cancer Sci.* **101,** 836–842
20. Morel-Huaux, V. M., Pypaert, M., Wouters, S., Tartakoff, A. M., Jurgan, U., Gevaert, K., and Courtoy, P. J. (2002) *Eur. J. Cell Biol.* **81,** 87–100
21. Lin, P., Le-Niculescu, H., Hofmeister, R., McCaffery, J. M., Jin, M., Hennemann, H., McQuistan, T., De Vries, L., and Farquhar, M. G. (1998) *J. Cell Biol.* **141,** 1515–1527
22. Lin, P., Yao, Y., Hofmeister, R., Tsien, R. Y., and Farquhar, M. G. (1999) *J. Cell Biol.* **145,** 279–289
23. Miura, K., Kurosawa, Y., and Kanai, Y. (1994) *Biochem. Biophys. Res. Commun.* **199,** 1388–1393
24. Gilchrist, A., Au, C. E., Hiding, J., Bell, A. W., Fernandez-Rodriguez, J., Lesimple, S., Nagaya, H., Roy, L., Gosline, S. J., Hallett, M., Paiement, J., Kearney, R. E., Nilsson, T., and Bergeron, J. J. (2006) *Cell* **127,** 1265–1281
25. Lin, P., Fischer, T., Weiss, T., and Farquhar, M. G. (2000) *Proc. Natl. Acad. Sci. U.S.A.* **97,** 674–679
26. Weiss, T. S., Chamberlain, C. E., Takeda, T., Lin, P., Hahn, K. M., and Farquhar, M. G. (2001) *Proc. Natl. Acad. Sci. U.S.A.* **98,** 14961–14966
27. Lin, P., Fischer, T., Lavoie, C., Huang, H., and Farquhar, M. G. (2009) *Mol. Neurodegener.* **4,** 15
28. Gump, J. M., June, R. K., and Dowdy, S. F. (2010) *J. Biol. Chem.* **285,** 1500–1507
29. Garcia-Marcos, M., Ghosh, P., Ear, J., and Farquhar, M. G. (2010) *J. Biol. Chem.* **285,** 12765–12777
30. Stols, L., Gu, M., Dieckman, L., Raffen, R., Collart, F. R., and Donnelly, M. I. (2002) *Protein Expr. Purif.* **25,** 8–15
31. Studier, F. W. (2005) *Protein Expr. Purif.* **41,** 207–234
32. De Vries, L., Elenko, E., McCaffery, J. M., Fischer, T., Hubler, L., McQuistan, T., Watson, N., and Farquhar, M. G. (1998) *Mol. Biol. Cell* **9,** 1123–1134
33. Austin, R. J., Ja, W. W., and Roberts, R. W. (2008) *J. Mol. Biol.* **377,** 1406–1418
34. de Alba, E., and Tjandra, N. (2004) *Biochemistry* **43,** 10039–10049
35. Mukhopadhyay, S., and Ross, E. M. (2002) *Methods Enzymol.* **344,** 350–369
36. Cuppen, E., van der Linden, A. M., Jansen, G., and Plasterk, R. H. (2003) *Comp. Funct. Genomics* **4,** 479–491
37. Welch, E. J., Jones, B. W., and Scott, J. D. (2010) *Mol. Interv.* **10,** 86–97

38. Coleman, D. E., Berghuis, A. M., Lee, E., Linder, M. E., Gilman, A. G., and Sprang, S. R. (1994) *Science* **265,** 1405–1412
39. Noel, J. P., Hamm, H. E., and Sigler, P. B. (1993) *Nature* **366,** 654–663
40. Denker, B. M., Schmidt, C. J., and Neer, E. J. (1992) *J. Biol. Chem.* **267,** 9998–10002
41. Woulfe, D. S., and Stadel, J. M. (1999) *J. Biol. Chem.* **274,** 17718–17724
42. Shu, F. J., Ramineni, S., Amyot, W., and Hepler, J. R. (2007) *Cell. Signal.* **19,** 163–176
43. Mittal, V., and Linder, M. E. (2004) *J. Biol. Chem.* **279,** 46772–46778
44. Webb, C. K., McCudden, C. R., Willard, F. S., Kimple, R. J., Siderovski, D. P., and Oxford, G. S. (2005) *J. Neurochem.* **92,** 1408–1418
45. McCudden, C. R., Willard, F. S., Kimple, R. J., Johnston, C. A., Hains, M. D., Jones, M. B., and Siderovski, D. P. (2005) *Biochim. Biophys. Acta* **1745,** 254–264
46. Kimple, R. J., Willard, F. S., Hains, M. D., Jones, M. B., Nweke, G. K., and Siderovski, D. P. (2004) *Biochem. J.* **378,** 801–808
47. Kapoor, N., Gupta, R., Menon, S. T., Folta-Stogniew, E., Raleigh, D. P., and Sakmar, T. P. (2010) *J. Biol. Chem.* **285,** 31647–31660
48. Willard, F. S., and Siderovski, D. P. (2006) *Biochem. Biophys. Res. Commun.* **339,** 1107–1112